

# Chapter 9

## Analysis of Drug Active Pharmaceutical Ingredients and Biomolecules Using Triple Quadrupole ICP-MS

Naoki Sugiyama and Yasuyuki Shikamori

**Abstract** Triple quadrupole ICP-MS (ICP-QQQ) can measure heteroatoms such as sulfur (S), phosphorus (P), and chlorine (Cl) at much lower levels than previously possible, making it highly suitable for the measurement of molecular compounds in life science research, including drug development. The tandem MS (MS/MS) configuration of the instrument, with a quadrupole positioned either side of the reaction cell, allows for much better control of any ion-molecular reactions that take place in the cell compared to conventional, single quadrupole ICP-QMS. As a number of molecular compounds of interest in life science research contain S, P, or Cl heteroatoms, the superior control of interferences provided by ICP-QQQ for the measurement of these challenging elements at trace levels was evaluated. The samples analyzed included drug active pharmaceutical ingredients (APIs) and peptide/phosphor peptides.

**Keywords** API • Active pharmaceutical ingredient • Drug analysis • Protein quantification • Phosphor peptide quantification • ICP-QQQ • ICP-MS/MS • Reaction cell

### 9.1 Introduction

In this chapter, the relatively new technique of triple quadrupole ICP-MS (ICP-QQQ) is described. Details are also given for the measurement of drug active pharmaceutical ingredients (APIs) and biomolecules such as proteins and phospho-proteins using the heteroatoms contained in the compounds. The improved detection capability of ICP-QQQ promises to make it the most suitable ICP-MS for life science research.

---

N. Sugiyama (✉) • Y. Shikamori  
Agilent Technologies International Japan, Ltd., 9-1 Takakura-cho, Hachioji, Tokyo 192-0033,  
Japan  
e-mail: [naoki\\_sugiyama@agilent.com](mailto:naoki_sugiyama@agilent.com)

With its high elemental and species-independent sensitivity, wide dynamic range, isotopic analysis capability, and high matrix tolerance, ICP-MS is already used by some life science researchers. Organic compounds that contain an ICP-MS detectable element can be quantified at trace levels on the basis of the compound's known stoichiometry. ICP-MS has been used in a number of studies regarding metalloproteins, which play a pivotal role in living organisms. Examples include metallothionein [1–3], superoxide dismutase (SOD) [4, 5], and ceruloplasmin [6] which contains copper (Cu) and/or zinc (Zn). The exceptional sensitivity of recent ICP-MS instrumentation has led to detection limits in the femtogram (fg)/g (ppq) range for elements with a mass number higher than 80. These elements tend to be relatively free from spectral interferences. The high sensitivity of ICP-MS has also been used to advantage to measure anticancer drug APIs and metabolites like cisplatin, which contains platinum (Pt) [7–9], as well as alternative drug candidates that contain ruthenium (Ru) [10, 11], which are expected to have less severe side effects.

For compounds that don't contain a metal/metalloid element, a "tagging" technique has been developed, where ICP-detectable elements such as iodine (I) [12], selenium (Se) [13], lanthanides [14, 15], or gold (Au) nanoparticles [16] are added into the target compound. The "tag" element is then detected by ICP-MS allowing the compound to be quantified. Tanner et al. [17] developed a novel technique to profile proteins in a single cell. A reagent was used to introduce different lanthanides to multiple target proteins using immunoassay. The profile of each protein in the cell was then obtained by measuring the lanthanides by ICP-MS. However, the complex process required to introduce the tag into target compound, possible different bioavailability of the tag-added compound from the original, or concern about tag introduction efficiency that must be high for accurate quantification are drawbacks of the technique.

A more straightforward approach to measure metal/metalloid-free compounds is to utilize a hetero element such as S, P, Cl, or Br as a natural tag. A number of proteins and peptides contain S, which is present in two proteinogenic amino acids: cysteine and methionine. Nucleic acids such as RNA and DNA contain P, and many drug APIs contain S, P, or halogens like Cl. It is a challenge for conventional ICP-QMS to measure these nonmetal elements at trace levels because of their low ionization rates (due to their high ionization potentials) and significant spectral interferences. However, ICP-QQQ, with its excellent spectral interference removal capability using MS/MS mode, allows the measurement of S, P, and Cl at much lower levels. Using this approach, it is possible to measure and quantify compounds via a heteroatom, without the need to introduce an artificial tag into the compound.

Quantitative analysis is one of the most valuable attributes of ICP-MS. For the technique to be more widely adopted by life science researchers, quantitative analysis of target compounds needs to be both accurate and simple. Due to the high temperature of the ICP ion source, compounds are readily atomized. Consequently, the sensitivity of ICP-MS is relatively matrix and compound independent compared to LC-MS, which is, in general, the first choice MS technique used in "omics" studies. While the high-temperature plasma ion source of ICP-MS doesn't

provide species information, unlike LC-MS, it does provide species-independent elemental sensitivity, which may allow compound quantitation without the need for compound-specific calibration standards. Life science applications including drug development studies are an emerging and interesting field for ICP-MS, especially for ICP-QQQ that can measure more organic compounds directly than conventional ICP-QMS.

## 9.2 ICP-QQQ

### 9.2.1 ICP-QQQ

Most current single quadrupole ICP-QMS instruments are fitted with a collision/reaction cell (CRC) in order to resolve spectral interferences. Although ICP-QMS can be used without a cell gas (called no gas mode), introducing a suitable gas into the cell removes or, at least, alleviates spectral interferences and improves detection limits. Interferences are reduced either by “collision” or “reaction” with a gas within the cell, hence the term collision/reaction cell.

Operating the CRC in collision mode using an inert gas such as helium (He) ensures that the analyte ion is discriminated from the interfering ion based on the difference of their ionic cross section. An interfering polyatomic ion is generally larger than the interfered analyte ion. For example,  $^{40}\text{Ar}^{35}\text{Cl}^+$  is larger than  $^{75}\text{As}^+$  and undergoes a greater number of collisions in the cell. As each collision causes energy loss, the interfering polyatomic ions lose more energy than the analyte ions and are subsequently filtered from the mass spectrum. This is achieved by discriminating between the two different energies using a process known as kinetic energy discrimination (KED). A different voltage is applied to the quadrupole and cell, so lower energy polyatomic ions cannot pass the potential barrier [18]. Helium collision mode is commonly used in general applications due to its universal effectiveness in interference removal and ease of use. Also, in contrast to reactive gases, helium collision mode doesn't require application-specific optimization. However, the improvement in signal-to-noise (interference) ratio is typically limited to one or two orders of magnitude, and He mode is largely ineffective for interferences caused by atomic isobars and doubly charged ions.

An alternative approach is to use reaction chemistry in the CRC of an ICP-QMS. However, since all ions formed in the plasma enter the reaction cell of a single quadrupole system, the reaction chemistry is uncontrolled, often leading to erroneous analytical results. Using a quadrupole ion guide as a dynamic reaction cell to prevent low-mass ions from entering the cell has been successful in some applications [19, 20], but not in all cases [21, 22].

The full potential of reaction cell chemistry can only be realized by ICP-QQQ which uses an additional quadrupole MS (Q1) in front of the CRC to control which ions can enter the cell and react. The second quadrupole (Q2, positioned after the

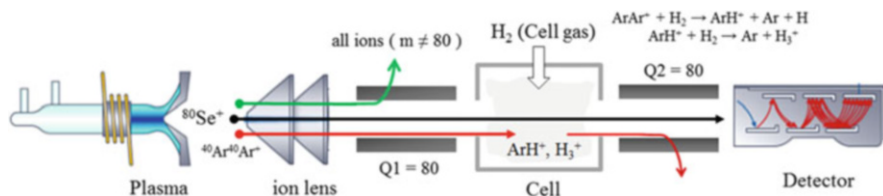


**Fig. 9.1** ICP-QQQ operation in on-mass mode to remove  $^{40}\text{Ar}^{40}\text{Ar}^+$  interference on  $^{80}\text{Se}^+$

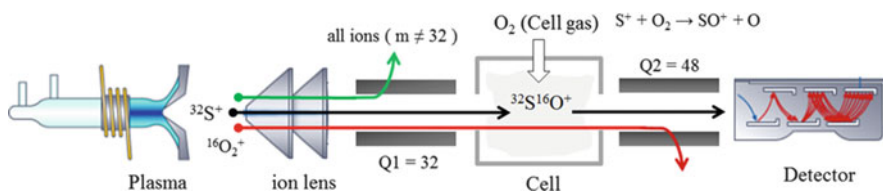


**Fig. 9.2** ICP-QQQ operation in mass-shift mode to remove  $^{16}\text{O}_2^+$  interference on  $^{32}\text{S}^+$

cell) selects the analyte ions that are passed to the detector. This double mass selection (MS/MS) is the fundamental reason for the superior control of interferences provided by ICP-QQQ. The configuration corresponds to the IUPAC definition of a triple quadrupole MS, as shown in Figs. 9.1 and 9.2. That is:

A tandem mass spectrometer comprising two transmission quadrupole mass spectrometers in series, with a (non-selecting) RF-only quadrupole (or other multipole) between them to act as a collision cell: [23]

The CRC consists of a series of lenses and a multipole RF ion guide which has multiple independent cell gas flow control systems. For example, the Agilent 8800 ICP-QQQ uses an octopole RF ion guide with a four-channel cell gas flow system used for the introduction of He (collision) gas and three reaction gases: hydrogen ( $\text{H}_2$ ), oxygen ( $\text{O}_2$ ), and ammonia ( $\text{NH}_3$ ). Each gas can be used alone or as mixture (mixed in the cell). Q1 can be operated as a simple ion guide (strictly speaking, a mass filter with the wide mass window) or as a 1-amu window mass filter. The former setting is referred to as single quadrupole scan mode and is used for conventional operation in no gas or He collision mode, emulating ICP-QMS. The latter setting is known as MS/MS scan mode and is used with a reactive cell gas. Using Q1 to select which ions enter the cell based on their mass-to-charge ratio ( $m/z$ ) ensures that the reactions within the cell are controlled and relatively sample independent. Consequently, ICP-QQQ with MS/MS has opened up new possibilities for analysts to address more applications using controlled reaction chemistry.

## 9.2.2 How MS/MS Works with a Reaction Gas

There are two types of reaction gas cell methods available with ICP-QQQ: *on-mass* where the setting of both quadrupoles is the same ( $Q1 = Q2$ ) and *mass shift* ( $Q1 \neq Q2$ ). The choice of method depends on the difference in the chemical reactivity (reaction rate) between the interfering ion and the analyte ion with the cell gas.

When the interfering ion reacts readily with the cell gas, it is removed from its original  $m/z$  at a faster rate than the analyte ion. The analyte ion can then be measured “on-mass” at its true isotope mass, free from interference. An example of the on-mass method is given in Fig. 9.1, which illustrates how  $^{80}\text{Se}$  is measured using  $\text{H}_2$  cell gas to remove the interference from  $^{40}\text{Ar}^{40}\text{Ar}^+$ .  $\text{ArAr}^+$  reacts quickly with  $\text{H}_2$  to form  $2\text{Ar} + \text{H}_3^+$ , while  $\text{Se}^+$  has a relatively low reaction rate with  $\text{H}_2$ . In this way,  $^{80}\text{Se}$  can be measured using  $\text{H}_2$  cell gas via mass pair of  $(Q1, Q2) = (80, 80)$ . The approach can also be used with ICP-QMS for the analysis of simple matrix samples. However, if bromine (Br) is present in the sample, as is often the case with bio fluid samples,  $^{79}\text{BrH}^+$  will form on reaction with  $\text{H}_2$  in the cell and interfere with  $^{80}\text{Se}^+$  at  $m/z$  80. This is not a problem with ICP-QQQ since all ions with  $m/z \neq 80$ , including  $^{79}\text{Br}^+$ , are rejected by Q1.

In contrast, mass shift is used when the analyte ion reacts readily with the reaction gas to form a new reaction product ion, while the interfering ion reacts slowly or not at all with the cell gas, so it does not contribute significantly to the signal at the new mass of the analyte product ion. An illustration is given in Fig. 9.2 using  $\text{O}_2$  cell gas to remove the  $^{16}\text{O}_2^+$  interference on  $^{32}\text{S}$ . The analyte ion  $\text{S}^+$  reacts with  $\text{O}_2$  to form  $\text{SO}^+$ , while the  $\text{O}_2^+$  interference reacts more slowly with  $\text{O}_2$ . Consequently,  $^{32}\text{S}$  can be measured with a dramatically improved S/N ratio as  $^{32}\text{SO}^+$  using  $\text{O}_2$  cell gas via mass pair of  $(Q1, Q2) = (32, 48)$ . If the background noise at the  $m/z$  of the product ion is low, even slow reaction rates between the analyte and cell gas to produce product ions will lead to a significant improvement in the S/N and detection limit (DL). Mass-shift mode is less suitable for ICP-QMS, which allows all ions formed in the plasma to enter the cell, including ions at the same  $m/z$  as any product ions. For example, if a sample contained calcium (Ca), titanium (Ti), or carbon (C) at high concentration, as in reverse phase LC-ICP-MS applications,  $^{48}\text{Ca}^+$ ,  $^{48}\text{Ti}^+$ , and  $^{36}\text{Ar}^{12}\text{C}^+$  would overlap the signal of the product ion  $^{32}\text{S}^{16}\text{O}^+$ , rendering the ICP-QMS method ineffective. With ICP-QQQ, in contrast, all of the potential interference ions ( $^{48}\text{Ca}^+$ ,  $^{48}\text{Ti}^+$  and  $^{36}\text{Ar}^{12}\text{C}^+$ ) would be removed by Q1. The differences between ICP-QQQ and ICP-QMS mass-shift methods are illustrated in Fig. 9.3 using the effect of Ca on the determination of S as an example. A mass spectrum of 2 ppb S was acquired with and without 50 ppb Ca, using  $\text{O}_2$  mass shift with MS/MS and single quad scan to emulate conventional ICP-QMS. It can be seen that  $^{32}\text{SO}^+$  suffers from a large positive error by the overlap from Ca in single quad scan mode, while MS/MS provides a theoretically matched isotopic pattern for S without any influence from Ca.

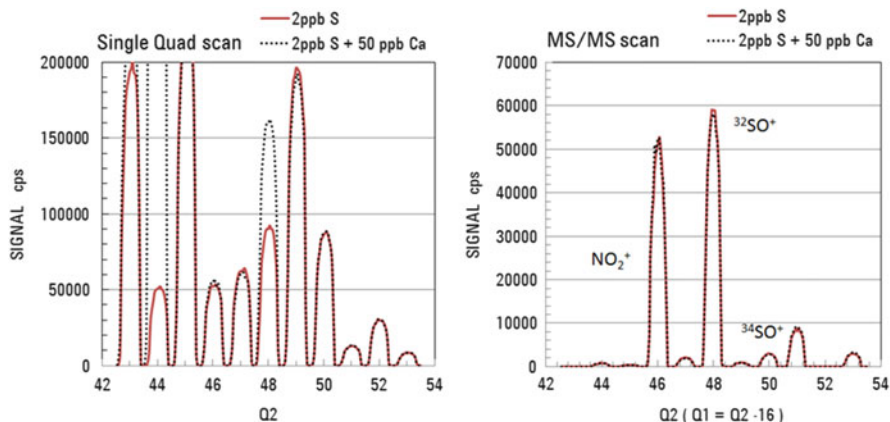


**Fig. 9.3** Spectrum of 2 ppb sulfur acquired using  $O_2$  mass-shift mode with and without the presence of 50 ppb Ca. *Left* single quad scan mode, *right* MS/MS scan mode

### 9.2.3 Reaction Cell Gas Selection

The most common ion-molecular reactions observed in the CRC are given below (not classified by reaction mechanism). B and  $B_1 \cdot B_2$  represent cell gas molecules, and  $A^+$  is an analyte ion or interfering ion which may be polyatomic, doubly charged or an atomic isobar.

- Charge transfer:  $A^+ + B \rightarrow A + B^+$
- Atom transfer:  $A^+ + B_1 \cdot B_2 \rightarrow A^+ \cdot B_1 + B_2$
- Association:  $A^+ + B + C \rightarrow A^+ \cdot B + C$

Theoretically, the charge transfer reaction can proceed when  $IP(A) > IP(B)$ , where IP stands for ionization potential. Atom transfer is observed in condensation or hydrogen atom transfer reactions, which will proceed if the affinity of  $A^+$  toward  $B_1$  is greater than affinity of  $B_2$  toward  $B_1$ . Examples of atom transfer reactions using  $B_1 = O$  [24],  $B_1 = H$  [25], and  $B_1 = F$  [26] can be found in the literature. Association reaction is known as clustering. For the product ion  $A^+ \cdot B$  to be stable, it requires another collision with C to release excess energy before the product ion breaks up. C may be molecule of B or molecule of buffer gas, He. A number of atomic ions react with  $NH_3$ ,  $CO_2$ , or  $CH_4$  to form complex cluster ions in a sequence reaction:  $A^+ \cdot B_n$ ,  $n = 1, 2, 3 \dots$

A number of reaction gases have been investigated including hydrogen, oxygen [24], ammonia [27], methane [28], ethylene [29], methyl fluoride [30], methyl chloride [31], nitrogen [32], nitrous oxide [33], carbon oxide [34], carbon dioxide [29], and others. However, the three most commonly used and effective gases for ICP-MS/ICP-QQQ are  $H_2$ ,  $O_2$ , and  $NH_3$ .

**Hydrogen ( $H_2$ )**  $H_2$  is an effective reaction gas used in on-mass methods to remove argide interferences such as  $^{40}Ar^+$  on  $^{40}Ca^+$ ,  $^{38}ArH^+$  on  $^{39}K^+$ ,  $^{40}ArC^+$  on  $^{52}C^+$ ,  $^{40}ArO^+$

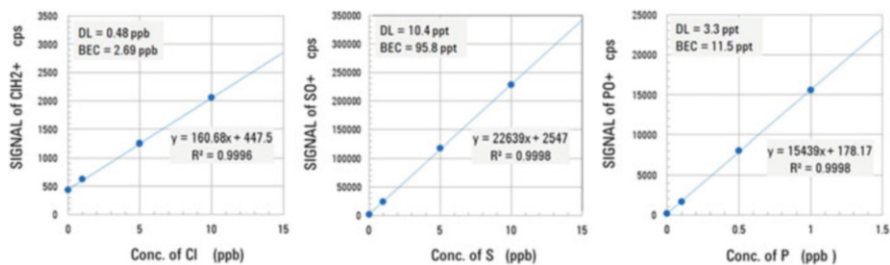


**Fig. 9.4** From the left, (a–c): (a) calibration curve of  $^{35}\text{Cl}$  in UPW acquired using ICP-QQQ in MS/MS mass-shift mode with  $\text{H}_2$  cell gas, octopole bias =  $-18$  V,  $\text{H}_2$  flow rate =  $5.0$  ml/min, KED =  $0$  V. (b) Calibration curve of  $^{32}\text{S}$  in UPW acquired using ICP-QQQ in MS/MS mass-shift mode with  $\text{O}_2$  cell gas: octopole bias =  $-3$  V,  $\text{O}_2$  flow rate =  $0.41$  ml/min, KED =  $-8$  V. (c) Calibration curve of  $^{31}\text{P}$  in UPW acquired using ICP-QQQ in MS/MS mass-shift mode with  $\text{O}_2$  cell gas: octopole bias =  $-3$  V,  $\text{O}_2$  flow rate =  $0.41$  ml/min, KED =  $-8$  V

on  $^{56}\text{Fe}^+$ ,  $^{40}\text{Ar}^{18}\text{OH}^+$  on  $^{59}\text{Co}^+$ ,  $^{40}\text{ArCl}^+$  on  $^{75}\text{As}^+$ , and  $^{40}\text{Ar}^{40}\text{Ar}^+$  on  $^{80}\text{Se}^+$ . Argide ions react with  $\text{H}_2$  at a relatively fast rate, while nearly all elemental ions exhibit low reactivity with  $\text{H}_2$ . However, a few applications use  $\text{H}_2$  effectively in mass-shift mode. An example is Cl analysis. Cl is a challenging element for ICP-QMS since both isotopes suffer intense interferences:  $^{35}\text{Cl}^+$  suffers an overlap from  $^{16}\text{O}^{18}\text{OH}^+$  and  $^{37}\text{Cl}^+$  suffers overlaps from  $^{36}\text{ArH}^+$ ,  $^{18}\text{O}^{18}\text{OH}^+$ , and  $(\text{H}_3\text{O})\text{H}_2\text{O}^+$ . However, as  $\text{Cl}^+$  reacts with  $\text{H}_2$  to form  $\text{ClH}_2^+$ ,  $^{35}\text{Cl}$  can be measured using ICP-QQQ in MS/MS mass shift with  $\text{H}_2$  via the mass pair of (Q1, Q2) = (35, 37). A calibration curve of  $^{35}\text{Cl}$  in ultrapure water (UPW) is shown in Fig. 9.4a. A DL of  $0.48$  ppb and back equivalent concentration (BEC) of  $2.69$  ppb were achieved.

**Oxygen ( $\text{O}_2$ )**  $\text{O}_2$  is highly suited to mass-shift methodology. A number of atomic ions react with  $\text{O}_2$  to form oxide ions by O-atom transfer. O-atom affinity of atomic ions is shown in Fig. 9.5, with the O-atom affinity of the O atom ( $5.2$  eV) indicated by the dotted line. Theoretically, atomic ions that have a higher O-atom affinity than the O atom react with  $\text{O}_2$  to form oxide ions. However, due to the contribution of collisional energy, atomic ions with a slightly lower O-atom affinity than the O atom actually form oxide ions in the reaction cell. Calibration curves of  $^{32}\text{S}$  and  $^{31}\text{P}$  in UPW obtained using  $\text{O}_2$  mass-shift mode are shown in Fig. 9.4b, c. DLs of  $10.4$  ppt and  $3.3$  ppt and BECs of  $95.8$  ppt and  $11.5$  ppt were obtained for S and P, respectively.

Another cell gas, nitrous oxide ( $\text{N}_2\text{O}$ ), is a more effective gas for O-atom transfer than  $\text{O}_2$ , since  $\text{N}_2$  has a lower O-atom affinity ( $1.6$  eV) than the O atom ( $5.2$  eV).  $\text{N}_2\text{O}$  reacts with more atomic ions to form oxide ions.

$\text{O}_2$  is also used in on-mass methods to remove interferences based on the oxide ions of refractory elements. Some of the oxide ions are highly reactive with  $\text{O}_2$  and are readily converted to dioxide and trioxide ions in the reaction cell. Unless the analyte ion reactivity toward  $\text{O}_2$  is also high, the element can be measured on-mass with the oxide ion interference removed or reduced. The method is suitable to



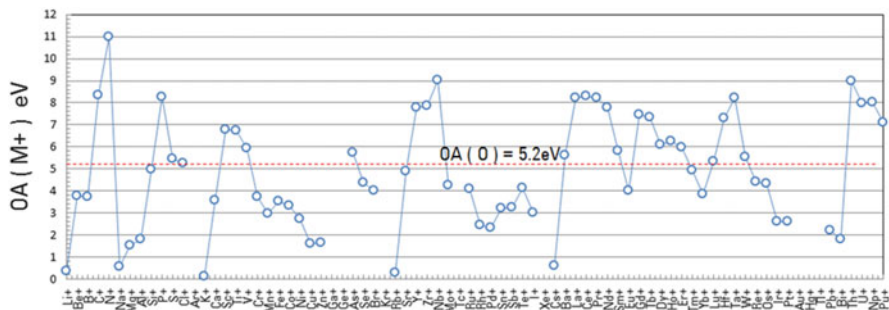
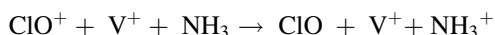


Fig. 9.5 O-atom affinity of atomic ions

resolve the molybdenum oxide ion ( $\text{MoO}^+$ ) interference on cadmium ( $\text{Cd}$ ) and zirconium oxide ion ( $\text{ZrO}^+$ ) overlap on silver ( $\text{Ag}$ ). Neither  $\text{Cd}^+$  nor  $\text{Ag}^+$  react readily with  $\text{O}_2$ , while neither  $\text{MoO}^+$  [35] nor did  $\text{ZrO}^+$  [36] react at a fast rate to be effectively converted to dioxide and trioxide ions.

**Ammonia ( $\text{NH}_3$ )**  $\text{NH}_3$  is highly reactive due to its lone electron pair. With an IP of 10.2 eV, which is lower than other common cell gases such as  $\text{H}_2$  (15.4 eV) and  $\text{O}_2$  (12.1 eV),  $\text{NH}_3$  is more likely to resolve an interference via a charge-exchange reaction. One example is the removal of  $^{35}\text{Cl}^{16}\text{O}^+$  interference on  $^{51}\text{V}^+$ . In the reaction cell filled with  $\text{NH}_3$ ,  $\text{ClO}^+$  (IP of  $\text{ClO} = 10.9$  eV) loses its charge via a charge-exchange reaction, while  $\text{V}^+$  analyte ions (IP of  $\text{V} = 6.74$  eV) remain mostly unaffected:



$\text{NH}_3$  is also an effective reaction gas to be used in mass-shift methods. The approach is often very versatile, although method development is more complex than on-mass methodology.  $\text{NH}_3$  reacts with many atomic ions,  $\text{M}^+$ , to form various product ions, described as  $\text{M}^+(\text{NH}_n)(\text{NH}_3)_m$ , where  $n = 0, 1, 2$  and  $m = 0, 1, 2, 3 \dots$ , via condensation and association reaction mechanisms. As long as there is a product ion that is free from interference, the product ion can be used to measure the analyte. Balcaen et al. [37] applied ICP-QQQ  $\text{NH}_3$  mass-shift to the measurement of trace titanium ( $\text{Ti}$ ) in blood and serum. All interferences on  $^{48}\text{Ti}^+$ , including the most challenging atomic isobaric overlap by  $^{48}\text{Ca}$ , were resolved by measuring product ion  $\text{Ti}(\text{NH}_3)_6^+$ .  $\text{NH}_3$  mass-shift methods can be very powerful when combined with the MS/MS capability of ICP-QQQ. Without the first quadrupole mass filter (Q1) available to remove any undesired precursor ions, coexisting elements in the sample would react with  $\text{NH}_3$  to produce a number of cluster product ions, some of which would likely overlap with the analyte product ion to be measured.



### 9.3 Application of ICP-QQQ for Drug API Analysis and Life Science Research

ICP-QQQ is expected to complement LC-MS in “omics” studies to provide a means for simpler and more accurate quantitative analysis. With drastically improved sensitivity and ability to determine challenging elements, ICP-QQQ is opening up more application opportunities for analysts.

#### 9.3.1 Drug API Analysis by LC-ICP-QQQ

Identification and quantification of drug APIs and metabolites are key tasks carried out during the many stages of drug development, including QA/QC. LC-MS is widely used for these applications. When the API is a metal-containing compound such as cisplatin, ICP-MS has also been used due to its unrivaled sensitivity to platinum (Pt). For the analysis of compounds containing more challenging elements such as S, P, and Cl at trace levels, ICP-QQQ can be used. Raeve et al. [38] applied ICP-QQQ to the absolute quantification of a molecular-targeted drug, trastuzumab. Trastuzumab is a monoclonal antibody (mAb) with a molecular mass of 148,000, comprising 44 sulfur atoms. The API sample was microwave-digested and was quantified using an isotope dilution (ID) method via  $^{34}\text{S}$ -enriched  $\text{H}_2\text{SO}_4$  spiked into the sample. A recovery of 97.8 % of the expected concentration was reported. Quantification of the API was achieved without the need for compound-specific calibration standards, unlike the general quantification method using LC-MS.

Drug development is an involved process which requires *in vitro* or *in vivo* studies including fundamental chemical characterization, toxicology tests, pharmacokinetic studies, bioavailability tests, etc. Each study would benefit from a faster, simpler, and more accurate technique for the quantification of the drug candidate API and/or the metabolites, all attributes of ICP-QQQ. A feasibility study of the analysis of drug APIs by LC-ICP-QQQ was carried out.

Three sulfonamide drug APIs, sulfamethizole, sulfamethazine, and sulfamethoxazole, were analyzed using LC-ICP-QQQ. The drugs are used for the treatment of bacterial infections as they inhibit the synthesis of bacterial folate that is essential for DNA synthesis in bacteria. Each sulfonamide is a small molecule, which contains one or two S atoms, and has a molecular mass of 250 – 280 Da. For the identification of the APIs, an HPLC (Agilent 1260 infinity bio-inert HPLC) fitted with a reverse phase (RP) column (Agilent ZORBAX plus C18 2.1 × 100 mm) was coupled to an ICP-QQQ (Agilent 8800). The ICP-QQQ was equipped with a narrow injector torch (1.5 mm id injector). An optional gas (20 % oxygen in Ar) was added to the same injector gas flow used for the organic solvent LC mobile phase to prevent carbon buildup on the interface cones. An isocratic mobile phase consisting of 13 % acetonitrile with 0.1 % formic acid was used at a flow rate of 0.4 ml/min. The injection volume was 20  $\mu\text{l}$ . An  $\text{O}_2$  mass-shift method for ICP-QQQ was

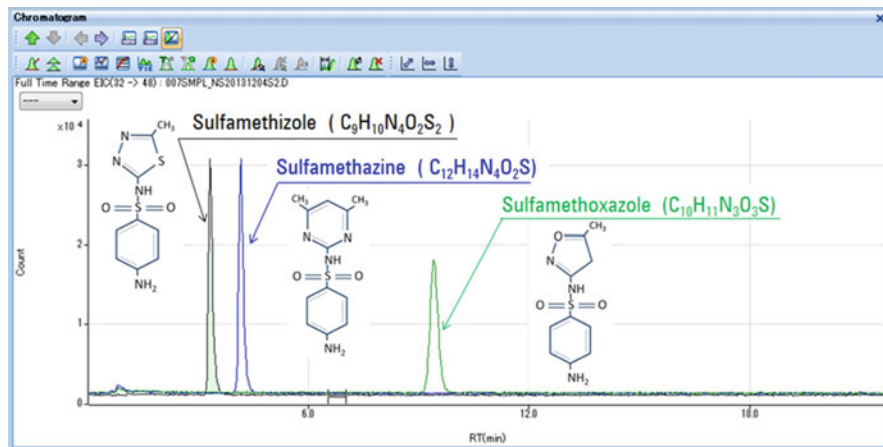


**Fig. 9.6** Chromatogram of sulfonamide drugs using reverse phase LC-ICP-QQQ. Sample contains S drug APIs at a concentration of 100 ppb (as S)

optimized to detect S contained in the sulfonamides using the following parameters:  $O_2$  cell gas flow rate = 0.3 ml/min, octopole bias =  $-4.0$  V, and KED voltage =  $-8.0$  V. From the chromatogram shown in Fig. 9.6, each API was identified via its retention time. The method detection limit for the compound sulfamethizole was calculated to be 23 nM (6.3 ppb as the compound and 1.5 ppb as the element S).

A similar approach (using the same configuration) was used to measure P- and Cl-containing drug APIs in two commercial drugs: ZOMETA® and Catapres®. ZOMETA® comprises a P-containing API and zoledronic acid monohydrate ( $C_5H_{10}N_2O_7P_2 \cdot H_2O$ ). The drug is used for the treatment of hypercalcemia (high level of blood calcium). The compound was identified and quantified via its P content using anion ion-pair LC-ICP-QQQ. P, as well as S, and can be measured using an  $O_2$  mass-shift method via a mass pair of  $(Q1, Q2) = (31, 47)$ . Figure 9.7 shows the calibration curve and a chromatogram of the sample. The isocratic LC mobile phase consisted of a 70:30 mixture of A: 6 mM tetra-butyl-ammonium bromide and 5 mM acetic acid adjusted to pH 6.5 with  $NH_3(aq)$  and B: 95% MeOH. The sample was prepared by diluting a 5 ml vial of commercially supplied ZOMETA® (which contained 4.264 mg of the API) by 2000-fold with the LC mobile phase. A five-point calibration curve from 100  $\mu g/l$  (ppb) to 2 mg/l (ppm) was prepared using a zoledronic acid monohydrate standard purchased from Sigma-Aldrich (St. Louis, MO, US). From the calibration, the concentration of the API was determined to be 433 ng/ml, equating to a recovery of 102%. The MDL for the drug compound was calculated to be 25 nM (144  $\mu g$ , 7.2 ppb as the compound and 1.5 ppb as the element P).

Catapres® is a commercial drug used for the treatment of hypertension. Its API is a Cl-containing compound, clonidine hydrochloride ( $C_9H_9Cl_2N_3 \cdot HCl$ ). The drug API was identified and quantified using RP-HPLC-ICP-QQQ to measure Cl. Figure 9.8 shows the calibration curve and chromatogram of the analysis. As

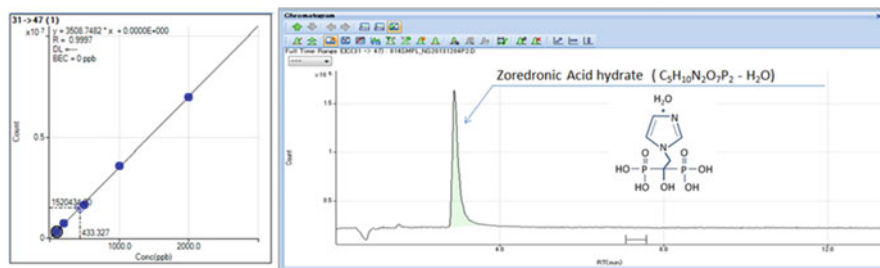


Fig. 9.7 Chromatogram of a P-containing drug API using LC-ICP-QQQ

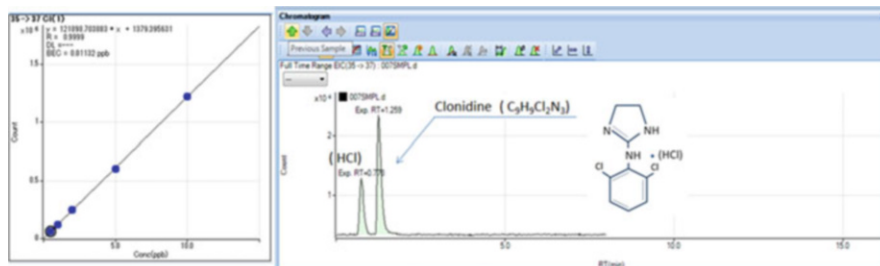


Fig. 9.8 Chromatogram of a Cl-containing drug API using LC-ICP-QQQ

mentioned previously, mass-shift mode using  $H_2$  cell gas is recommended for Cl analysis via a mass pair of  $(Q1, Q2) = (35, 37)$ .  $Cl^+$  ( $m/z$  35) is converted to  $ClH_2^+$  ( $m/z$  37) via reaction with  $H_2$  cell gas at 3 ml/min flow rate. An isocratic mobile phase of 20% acetonitrile with 0.1% formic acid was used. A tablet of Catapres® (containing 75  $\mu g$  of the API) was dissolved in 50 ml ultrapure water (Organo PURIC- $\omega$ ), sonicated for 60 min, filtered with a 0.2  $\mu m$  filter, and injected into the LC as a sample. A calibration curve was prepared by analyzing clonidine hydrochloride standards purchased from Sigma-Aldrich (St. Louis, MO, US). The concentration of the API was found to be 1444 ng/ml, which is a recovery of 96%. The MDL for the drug compound was calculated to be 146 nM (780 pg, 39 ppb as compound and 15 ppb as the element Cl).

### 9.3.2 Peptide and Phosphor Peptide Analysis by Capillary-LC-ICP-QQQ

The objective of life science research is to find ever more suitable treatments for disorders. Several “omics” research fields have developed according to the kind of compound the research targets: genomics, transcriptomics, proteomics,

metabolomics, and metallomics. A number of research themes are ongoing around the world to elucidate the cause or the pathway of various diseases and to finally find effective remedies. In omics studies, LC-MS is widely used for the identification, structural analysis, and quantification of target protein/peptides together with classical techniques like Western blot, ELISA, and modified techniques. However, the quantification of protein/peptides is still often challenging and ICP-MS is expected to fill the gap. The high-temperature plasma ionization source of ICP-MS provides an advantage over soft ionization sources such as ESI or MALDI of LC-MS, with its matrix-independent and species-independent sensitivity. The matrix-independent sensitivity of ICP-MS resolves, or at least alleviates, a well-known issue of ESI-MS, which is signal suppression by a co-eluting compound. As a result, ICP-MS provides a more accurate means of quantification of protein/peptides. The species-independent sensitivity of ICP-MS allows for compound-independent calibration (CIC), and CIC can be used to quantify even multiple protein/peptides using a single standard without the need for reference standards, which are often expensive or difficult to obtain.

A feasibility study has demonstrated the capability of ICP-QQQ for the analysis of protein/peptides and phosphor peptides [39]. Phosphorylation is one of the most important post transcript modification (PTM) components that plays a pivotal role in controlling the function of proteins in living organisms. Precise and accurate analysis of the PTM is of paramount importance in proteomics. As detailed previously, ICP-QQQ can measure protein/peptides and phosphor peptides via an S or P heteroatom. To do this, a micro-flow LC (Agilent 1200 series capillary LC) was coupled to an ICP-QQQ (Agilent 8800 with 1.5 mm id injector torch) via a total consumption nebulizer (Agilent G3680A), as shown in Fig. 9.9. The nebulizer was used with a specially designed single-pass spray chamber (not chilled), providing 100% sample introduction efficiency at the low LC flow rate. The LC was fitted with a micro-bore RP column (Agilent ZORBAX SB C18, 5  $\mu$ m, 0.3  $\times$  150 mm).

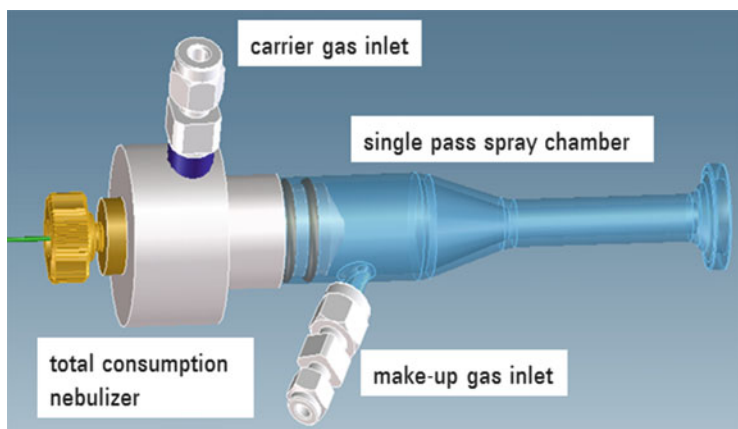


**Fig. 9.9** Illustration of total consumption nebulizer and single-pass spray chamber

The end of the column was connected directly to the total consumption nebulizer via a capillary tube. The mobile phases A and B consisted of water and acetonitrile containing 0.1% formic acid. A gradient flow was used at a flow rate of 5  $\mu$ l: 0–3 min A:B = 99:1 isocratic and 3–35 min A:B = 40:60 linear. The injection volume was 1  $\mu$ l. ICP-QQQ was used in O<sub>2</sub> mass-shift mode for the determination of S and P. The instrument was optimized by introducing 50% acetonitrile containing an inorganic sulfur standard and maximizing the SO<sup>+</sup> signal. Figure 9.10 shows a chromatogram of a sample containing two peptides and two phosphor peptides at a concentration of 45 ng/ml (as S and P). The sample also contains methionine and bis(4-nitrophenyl) phosphate (BNPP) as internal standards at a concentration of 105 ng/ml (as S and P). The sample peptides have amino acid sequences of ACTPERMAE and VPMLK, which contain the S-containing amino acid cysteine and/or methionine. The amino acid sequences of the sample phosphor peptides are LRRApSLG and KRSpYEEHIP, which contain phosphorylated serine and tyrosine, respectively. From the signal of the internal standard, the method DL was calculated to be 0.18 ng/ml as S and 0.10 ng/ml as P (11 fmol S and 6.6 fmol P). Future work will concentrate on the absolute quantification of peptide/phosphor peptides using CIC.

## 9.4 Conclusions

ICP-QQQ operating in MS/MS mode realizes the potential of using reactive cell gases to eliminate problematic spectral interferences. The first MS restricts which ions enter the cell, so that the reaction can be controlled, ensuring consistent and reliable reaction cell performance. Hence, elements considered challenging for conventional ICP-QMS, such as S, P, and Cl, can now be measured at lower levels using ICP-QQQ than previously possible. This provides more opportunities for the analysis of bio molecules in life science research and drug development processes,

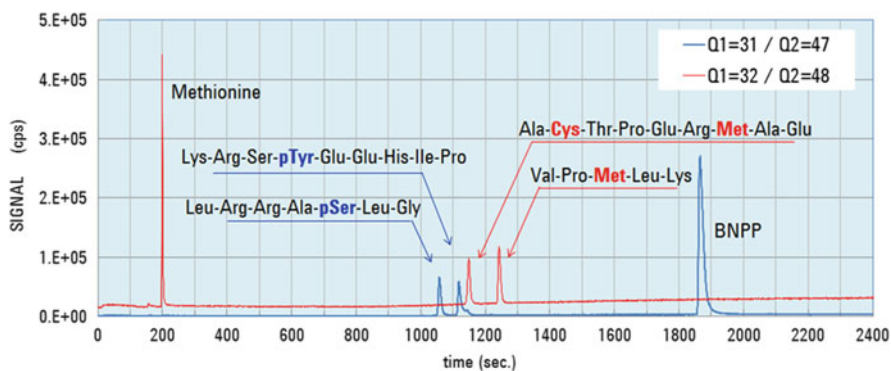


Fig. 9.10 Chromatogram of peptides and phosphor peptides using micro-flow LC-ICP-QQQ

since a number of the compounds of interest contain one of these heteroatoms. Due to the high-temperature ionization source, ICP-MS has an advantage in quantitative analysis over LC-MS as it provides simpler, faster, and more accurate quantitative analytical measurements. ICP-MS is expected to complement LC-MS for emerging life science research with ICP-QQQ becoming the technique of choice due to its superior detection capability of heteroatoms, while remaining applicable for conventional metals analysis, including the measurement of metal-tagged biomolecules.

To highlight the capabilities of ICP-QQQ for the analysis of drug APIs, S-, P-, and Cl-containing drug APIs were analyzed with excellent sensitivity using LC-ICP-QQQ. Drug development is a lengthy process comprising many stages. As ICP-QQQ provides improved quantitative analysis, the technique could contribute to more efficient and faster drug development. ICP-QQQ coupled with micro-flow LC was used to analyze peptides and phosphor peptides via the heteroatoms of S and P – again with good sensitivity. More widespread use of ICP-QQQ is expected in order to improve accuracy and sensitivity in quantitative analysis especially the degree of expressed protein or phosphorylation.

Future work will focus on the application of ICP-QQQ for actual research projects. To fully realize the advantage of ICP-MS in quantitative analysis, further study on compound-independent calibration (CIC) is needed in real applications. Quantifying biomolecules like proteins without the need for a standard compound would be of great benefit in life science research, including drug development. It remains a challenge currently to apply CIC generally, especially to gradient flow LC-ICP-MS, so this is an area of development.

## References

1. Murray K, Boyd R, Eberlin M (2013) IUPAC recommendation 2013. *Pure Appl Chem* 85 (7):1515–1609
2. Tanner SD, Baranov VI, Bandura DR (2002) Reaction cells and collision cells for ICP-MS: a tutorial review. *Spectrochim Acta B* 57:1361–1452
3. Navaza A, Ruiz-Encinar J, Ballesteros A et al (2009) Capillary HPLC–ICPMS and tyrosine iodination for the absolute quantification of peptides using generic standards. *Anal Chem* 81:5390–5399
4. Ornatsky OI, Kinach R, Bandura DR et al (2008) Development of analytical methods for multiplex bio-assay with inductively coupled plasma mass spectrometry. *J Anal At Spectrom* 23:463–469
5. Agilent 8800 ICP-QQQ application handbook 5991-2802EN (2013):16–18
6. Tanner SD, Li C, Vais V et al (2004) Chemical resolution of Pu+ from U+ and Am+ using a band-pass reaction cell inductively coupled plasma mass spectrometer. *Anal Chem* 76:3042–3048
7. Quemet A, Vitorge P, Cimas A et al (2013) Reactivity of lanthanoid mono-cations with ammonia: a combined inductively coupled plasma mass spectrometry and computational investigation. *Int J Mass Spectrom* 334:27–37

8. Esteban-Fernández D, Bierkandt F, Linscheid M (2012) MeCAT labeling for absolute quantification of intact proteins using label-specific isotope dilution ICP-MS. *J Anal At Spectrom* 27:1701–1708
9. Vanhaecke F, Balcaen L, Deconinck I et al (2003) Mass discrimination in dynamic reaction cell (DRC)-ICP-mass spectrometry. *J Anal At Spectrom* 18:1060–1065
10. He Q, Zhu Z, Jin L et al (2014) Detection of HIV-1 p24 antigen using streptavidin–biotin and gold nanoparticles based immunoassay by inductively coupled plasma mass spectrometry. *J Anal At Spectrom* 29:1477–1482
11. Cheng P, Koyanagi GK, Bohme DK (2006) Gas-phase reactions of atomic lanthanide cations with CO<sub>2</sub> and CS<sub>2</sub>: room-temperature kinetics and periodicities in reactivity. *J Phys Chem A* 110(47):12832–12838
12. Corte Rodriguez M, López Fernández L, Garcia Fernandez A et al (2015) Elemental and molecular mass spectrometric strategies for probing interactions between DNA and new Ru(II) complexes containing phosphane ligands and either a tris(pyrazol-1-yl)borate or a pyridine bis (oxazoline) ligand. *J Anal At Spectrom* 30:172–179
13. Balcaen L, Bolea-Fernandez E, Resano M et al (2014) Accurate determination of ultra-trace levels of Ti in blood serum using ICP-MS/MS. *Anal Chim Acta* 809(27):1–8
14. Koyanagi GK, Baranov VI, Tanner SD et al (2000) An inductively coupled plasma/selected-ion flow tube mass spectrometric study of the chemical resolution of isobaric interferences. *J Anal At Spectrom* 15:1207–1210
15. Diez Fernández S, Sugiyama N, Ruiz-Encinar J et al (2012) Triple quad ICPMS (ICPQQQ) as a new tool for absolute quantitative proteomics and phosphoproteomics. *Anal Chem* 84:5851–5857
16. Sucharová J (2011) Optimisation of DRC ICP-MS for determining selenium in plants. *J Anal At Spectrom* 26:1756–1762
17. Moller LH, Gabel-Jensen C, Franzyk H et al (2014) Quantification of pharmaceutical peptides using selenium as an elemental detection label. *Metallomics* 6:1639–1647
18. Simpson LA, Thomsen M, Alloway BJ et al (2001) A dynamic reaction cell (DRC) solution to oxide-based interferences in inductively coupled plasma mass spectrometry (ICP-MS) analysis of the noble metals. *J Anal At Spectrom* 16:1375–1380
19. Bolea-Fernandez E, Balcaen L, Resano M et al (2015) Interference-free determination of ultra-trace concentrations of arsenic and selenium using methyl fluoride as a reaction gas in ICP-MS/MS. *Anal Bioanal Chem* 407:919–929
20. Chang C, Liu H, Jiang S (2003) Bandpass reaction cell inductively coupled plasma mass spectrometry for the determination of silver and cadmium in samples in the presence of excess Zr, Nb and Mo. *Anal Chim Acta* 493:213–218
21. Esteban-Fernández D, Verdaguer JM, Ramirez-Camacho R et al (2008) Accumulation, fractionation, and analysis of platinum in toxicologically affected tissues after cisplatin, oxaliplatin, and carboplatin administration. *J Anal Toxicol* 32(2):140–146
22. Lavrov VV, Blagojevic V, Koyanagi GK et al (2004) Gas-phase oxidation and nitration of first-, second-, and third-row atomic cations in reactions with nitrous oxide: periodicities in reactivity. *J Phys Chem A* 108:5610–5624
23. Bolea-Fernandez E, Balcaen L, Resano M et al (2014) Potential of methyl fluoride as a universal reaction gas to overcome spectral interference in the determination of ultratrace concentrations of metals in biofluids using inductively coupled plasma-tandem mass spectrometry. *Anal Chem* 86:7969–7977
24. Ferrarello C, Ruiz-Encinar J, Centineo G et al (2002) Comparison of three different ICP-MS instruments in the study of cadmium speciation in rabbit liver metallothionein-I using reversed-phase HPLC and post-column isotope dilution analysis. *J Anal At Spectrom* 17:1024–1029
25. Miyayama T, Ogra Y, Suzuki K (2007) Separation of metallothionein isoforms extracted from isoform-specific knockdown cells on two-dimensional micro high-performance liquid



- chromatography hyphenated with inductively coupled plasma-mass spectrometry. *J Anal At Spectrom* 22:179–182
26. Falta T, Heffeter P, Mohamed A et al (2011) Quantitative determination of intact free cisplatin in cell models by LC-ICP-MS. *J Anal At Spectrom* 26:109–115
  27. Campenhout KV, Infante HG, Adams F et al (2004) Induction and binding of Cd, Cu, and Zn to metallothionein in carp (*Cyprinus carpio*) using HPLC-ICP-TOFMS. *Toxicol Sci* 80:276–287
  28. Raeve P, Bianga J (2015) Fast and accurate absolute-quantification of proteins and antibodies using Isotope Dilution-Triple Quadrupole ICP-MS. Agilent Technologies application note 5991-6118EN
  29. Lelie H, Liba A, Bourassa M et al (2011) Copper and zinc metallation status of copper-zinc superoxide dismutase from amyotrophic lateral sclerosis transgenic mice. *J Biol Chem* 286 (4):2795–2806
  30. Hermann G, Heffeter P, Falta T et al (2013) In vitro studies on cisplatin focusing on kinetic aspects of intracellular chemistry by LC-ICP-MS. *Metallomics* 5(6):636–647
  31. Nuevo Ordóñez Y, Deitrich CL, Montes-Bayón M et al (2011) Species specific isotope dilution versus internal standardization strategies for the determination of Cu, Zn superoxide dismutase in red blood cells. *J Anal At Spectrom* 26:150–155
  32. Tayler VF, Evans RD, Cornett RJ (2007) Determination of <sup>90</sup>Sr in contaminated environmental samples by tuneable bandpass dynamic reaction cell ICP-MS. *Anal Bioanal Chem* 387:343–350
  33. Tanner SD, Bandura DR, Ornatsky O et al (2008) Flow cytometer with mass spectrometer detection for massively multiplexed single-cell biomarker assay. *Pure Appl Chem* 80 (12):2627–2641
  34. Martinčič A, Milačič R, Vidmar J et al (2014) New method for the speciation of ruthenium-based chemotherapeutics in human serum by conjoint liquid chromatography on affinity and anion-exchange monolithic disks. *J Chromatogr A* 1371:168–176
  35. Olesik JW, Jones DR (2006) Strategies to develop methods using ion-molecule reactions in a quadrupole reaction cell to overcome spectral overlaps in inductively coupled plasma mass spectrometry. *J Anal At Spectrom* 21:141–159
  36. Koyanagi GK, Caraiman D, Blagojevic V et al (2002) Gas-phase reactions of transition-metal ions with molecular oxygen: room-temperature kinetics and periodicities in reactivity. *J Phys Chem A* 106:4581–4590
  37. Olesik JW, Gray PJ (2014) Advantages of N<sub>2</sub> and Ar as reaction gases for measurement of multiple Se isotopes using inductively coupled plasma-mass spectrometry with a collision/reaction cell. *Spectrochim Acta B* 100:197–210
  38. Lopez-Avila V, Sharpe O, Robinson WH (2006) Determination of ceruloplasmin in human serum by SEC-ICPMS. *Anal Bioanal Chem* 386:180–187
  39. McCurdy E, Woods G (2004) The application of collision/reaction cell inductively coupled plasma mass spectrometry to multi-element analysis in variable sample matrices, using He as a non-reactive cell gas. *J Anal At Spectrom* 19:607–615